RESEARCH ON DISTURBANCE REJECTION CONTROL STRATEGY OF VEHICLE DRIVE AXLE LOADING TEST BENCH

Hui Yu, Hui Wang, Nanqi Li, Guochao Zhao

Liaoning Technical University, School of Mechanical Engineering, Fuxin, China
e-mail: wanghui9955@163.com

Aiming at the problems of parameter disturbance and coupling disturbance in a vehicle drive axle loading test-bed, this paper used the adaptive backstepping sliding mode control (ABSMC) strategy to design the controller for the speed and torque system. The effectiveness of the controller has been verified by simulation and an experiment. The results show that the equivalent moment of inertia is increased by 5 times, and the step response overshoot of the speed system is 4.1%. By adding a random disturbance, the sinusoidal tracking errors of the speed and torque systems are 0.05 r/min and 0.09 Nm, respectively.

Keywords: loading test-bed, disturbance, adaptive backstepping sliding mode control, overshoot, sinusoidal tracking error

1. Introduction

With the continuous improvement of people's requirements for vehicle reliability and operation performance, the research on simulated loading tests of vehicle key components has attracted more and more attention (Peng *et al.*, 2013). The performance of the vehicle largely depends on working characteristics of the vehicle engine and wheel axle, and the engine is often an established on-demand product. Therefore, it is particularly important to carry out simulated loading tests on the vehicle drive axle under various complex working conditions (Han *et al.*, 2009). The working environment of engineering vehicles is mostly poor, as a key component of the vehicle, the working performance of the drive axle determines the reliability and stability of the vehicle (Zhai *et al.*, 2016). Using a loading test bench to carry out the loading test on the drive axle indoors can evaluate the quality and reduce the development cost (Lauwerys *et al.*, 2005). In the recent years, due to the society's high promotion of energy conservation, emission reduction and efficient utilization, the development of low-carbon and energy-saving vehicles has attracted more and more attention (Fajri *et al.*, 2016). Because of its unique advantages, secondary regulation technology is more and more used in vehicle drive axle loading test-beds. Compared with the traditional hydrostatic transmission and electric transmission, the loading test equipment based on the secondary regulation technology has the advantages of better control performance, higher system efficiency and less power consumption (Shen *et al.*, 2017).

The precision control of the secondary regulation system has also received extensive attention. Ding *et al.* (2006) proposed a method combining dynamic matrix predictive control and PID. The inner loop is used to overcome the random interference, and the outer loop uses predictive control to obtain excellent tracking performance and robustness. Su and Wang (2006) based their research on the state space method. The control problem of a class of dual input single output speed system was studied, and a PID control strategy adjusted by a genetic algorithm was given. Hu *et al.* (2008), based on the principle of structural invariance, designed a feedforward compensation loop device for the speed control system to suppress the load interference. Zang *et al.* (2014) proposed a control method combining fuzzy logic and neural network. Zang *et*

al. (2016) also studied a robust control problem of the secondary regulation speed system by using the Hamiltonian function method. However, the speed and torque systems simulated by the wheel bridge loading test-bed are rigidly coupled through the loading object (Li *et al.*, 2014). In addition, there are many parameters and large changes in the system, resulting in a serious external coupling interference and internal parameter disturbance in the speed and torque systems (Li and Jia, 2017). Therefore, in order to improve the control accuracy of the loading test-bed, this paper combines an adaptive, backstepping and sliding mode algorithm to design the controller of the speed and torque systems. The internal uncertainty of the system is eliminated by sliding mode control (Song and Yu, 2020). Based on the backstepping sliding mode algorithm, the compensation control of the adaptive law is introduced to eliminate the influence of the external interference from the system through estimation (Huang and Yang, 2015).

2.   System principle

As shown in Fig. 1, the vehicle drive axle loading test system based on the secondary regulation technology is shown. Four sets of secondary elements are connected in parallel in a constant voltage network by pressure coupling. The other end is connected in one by mechanical coupling through speed and torque sensors, transmission and the wheel bridge. Secondary element 1 works under the motor condition and constitutes the driving speed control system with the speed sensor and controller 1. Secondary elements 2, 3 and 4 work under the pump condition, they form the secondary output loading the torque control system and the wheel side loading torque control system together with corresponding torque sensors and controllers 2, 3 and 4, respectively. Secondary element 1 (motor) converts hydraulic energy into mechanical energy to drive the loading object (wheel bridge) and secondary elements 2, 3 and 4 (pump) to realize simulated loading. Secondary elements 2, 3, 4 (pump) convert mechanical energy to hydraulic pressure and give back to the constant pressure network. Therefore, the loading system can realize energy recovery. Since the settings of the four sets of the secondary regulation systems are the same, any one of them can be set as the driving unit and the other one, two or three sets as the loading unit to form a 2-axis, 3-axis or 4-axis composite loading system.

Because the structure, components and parameters of the secondary output loading torque control system and the left and right wheel side loading torque control systems are the same, for the sake of simplification, this paper only studies the secondary output loading torque control system and the drive speed control system, hereinafter referred to as the torque system and the speed system.

According to the loading system shown in Fig. 1 and the system equation proposed by Wang *et al.* (2018), the state space equation of the speed system can be obtained as

$$
\begin{aligned}
&\dot{x}_1 = x_2 \qquad\quad \dot{x}_2 = x_3 \qquad\quad \dot{x}_3 = x_4 \\
&\dot{x}_4 = a_1 x_1 + a_2 x_2 + a_3 x_3 + a_4 x_4 + a_5 u + F_1 \\
&Y = x_1
\end{aligned}
\tag{2.1}
$$

where Y represents the speed output of the speed system, u is the control input

$$
a_1 = -\frac{\omega_v^2 K_v (K_y R_q Y_{max} + K_n V_{max} P_L)}{J_q A Y_{max}} \qquad a_2 = -\Big(\frac{\omega_v^2 K_v K_y}{A} + \frac{\omega_v^2 R_q}{J_q}\Big)
$$

$$
a_3 = -\Big(\omega_v^2 + \frac{2\omega_v \zeta_v}{J_q}\Big) \qquad a_4 = -\Big(2\omega_v \zeta_v + \frac{R_q}{J_q}\Big) \qquad a_5 = \frac{\omega_v^2 K_v V_{max} P_L}{A Y_{max}}
$$
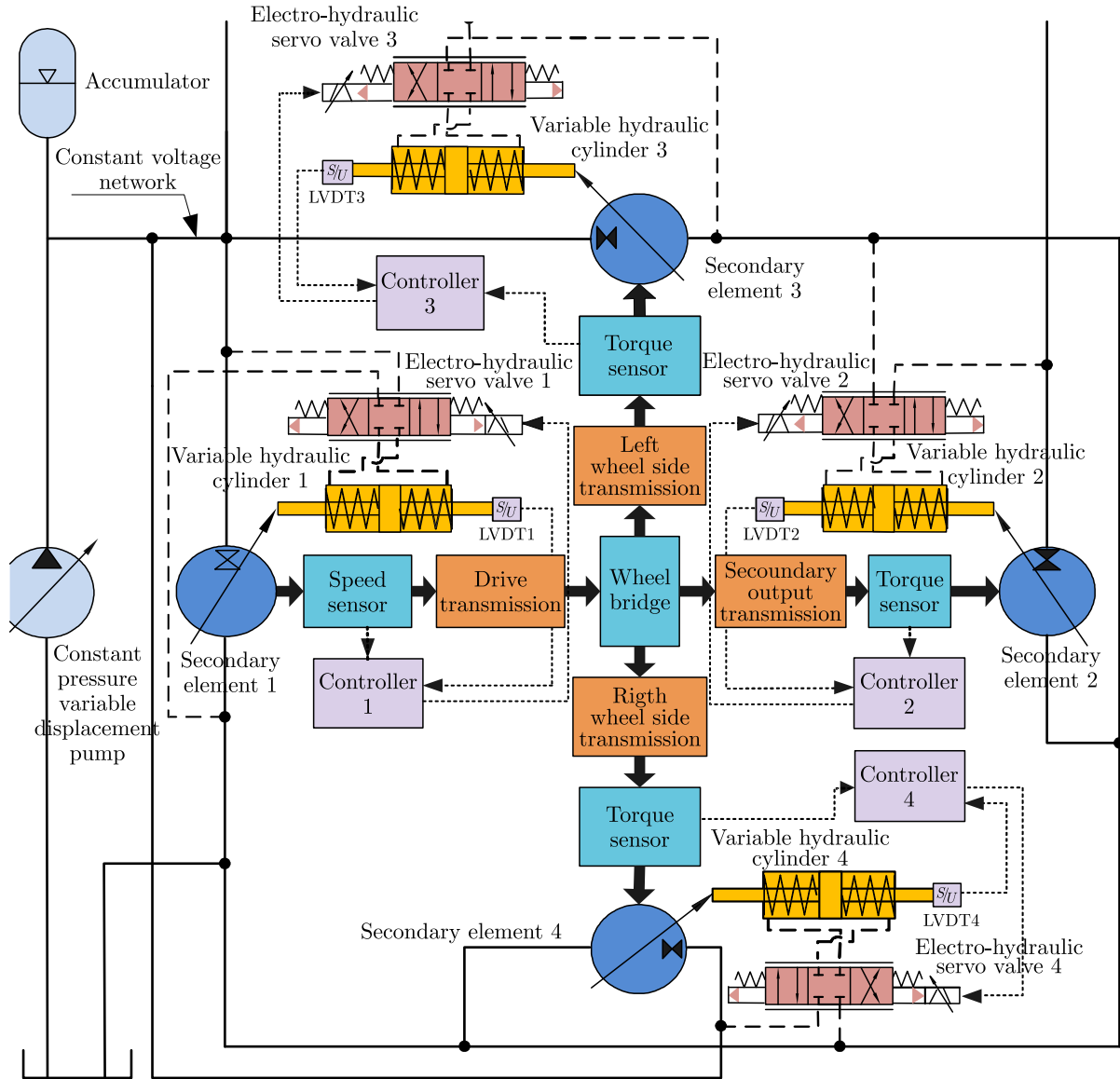
Fig. 1. Principle diagram of the simulation loading system

The state space equation of the torque system is

$$\dot{x}_1 = x_2 \qquad \dot{x}_2 = x_3 \qquad \dot{x}_3 = b_1 x_1 + b_2 x_2 + b_3 x_3 + b_4 u + F_2$$
$$Y = x_1 \tag{2.2}$$

where Y represents the torque output of the torque system, u is the control input

$$b_1 = -\frac{\omega_v^2 K_v (K_y Y_{max} + K_m V_{max} P_L)}{A Y_{max}} \qquad b_2 = -\omega_v^2$$

$$b_3 = -2\omega_v \zeta_v \qquad b_4 = \frac{\omega_v^2 K_v V_{max} P_L)}{A Y_{max}}$$

and F_1, F_2 are the uncertainty parameter and the coupling interference of the speed and torque systems, respectively. Other parameters in equations (2.1) and (2.2) are shown in Table 1.

Table 1. Main parameters of the system

Symbol	Description	Figure
J_q [kg m^2]	Equivalent moment of inertia of loading mechanical system	1.13
R_q [N m/(rad/s)]	Viscous damping coefficient of drive axle	0.22
K_v [(m^3/s)/v]	Flow gain of electro-hydraulic servo valve	$1.1 \cdot 10^{-4}$
ω_v [rad/s]	Natural frequency of electro-hydraulic servo valve	560
ζ_v [–]	Damping ratio of electro-hydraulic servo valve	0.5
A [m^2]	Effective area of variable pressure cylinder	$1.41 \cdot 10^{-3}$
Y_{max} [m]	Maximum displacement of piston of variable hydraulic cylinder	$2.63 \cdot 10^{-2}$
P_L [N/m^2]	Load pressure of variable hydraulic cylinder	$20.0 \cdot 10^6$
V_{max} [m^3/rad]	Maximum displacement of secondary element	$250.00 \cdot 10^{-6}$
k_y [–]	Transformation coefficient of displacement sensor	10
k_n, k_m [–]	Speed and torque sensor coefficients	0.01

3. Controller design of the speed and torque systems

According to equation (2.1), assuming that the control target is the speed output Y of the speed system, the tracking command is x_d and the first, second, third and fourth derivatives of x_d are derivable, the tracking error is

$$z_1 = Y - x_d \qquad \dot{z}_1 = \dot{Y} - \dot{x}_d = x_2 - \dot{x}_d \tag{3.1}$$

Define the first Lyapunov function

$$v_1 = \frac{1}{2}z_1^2 \qquad \dot{v}_1 = z_1 \dot{z}_1 \qquad \dot{z}_1 = z_1(x_2 - \dot{x}_d) \tag{3.2}$$

where

$$x_2 = -c_1 z_1 + \dot{x}_d + z_2 \qquad z_2 = x_2 + c_1 z_1 - \dot{x}_d \tag{3.3}$$

z_2 is the virtual control term, c_1 is a positive constant (Pang *et al.*, 2021)

$$\dot{v}_1 = -c_1 z_1^2 + z_1 z_2 \tag{3.4}$$

If $z_2 = 0$, then $\dot{v}_1 \leqslant 0$. And so on until the third Lyapunov function is defined as

$$v_3 = v_2 + \frac{1}{2}z_3^2$$
$$\dot{v}_3 = \dot{v}_2 + z_3 \dot{z}_3 = -c_1 z_1^2 - c_2 z_2^2 + z_2 z_3 + z_3(x_4 + c_1 \ddot{z}_1 - \dddot{x}_d + c_2 \dot{z}_2 + \dot{z}_1) \tag{3.5}$$

where

$$z_4 = x_4 + c_3 z_3 + z_2 + c_1 \ddot{z}_1 - \dddot{x}_d + c_2 \dot{z}_2 + \dot{z}_1 \tag{3.6}$$

c_3 is a positive constant, z_4 is a virtual control term

$$\dot{v}_3 = -c_1 z_1^2 - c_2 z_2^2 - c_3 z_3^2 + z_3 z_4 \tag{3.7}$$

Define the sliding mode switching function

$$\delta_n = k_1 z_1 + k_2 z_2 + k_3 z_3 + z_4 \tag{3.8}$$

The Lyapunov function is defined as follows

$$v_4 = v_3 + \frac{1}{2}\delta_n^2$$

$$\begin{aligned}\dot{v}_4 &= \dot{v}_3 + \delta_n\dot{\delta}_n = -c_1 z_1^2 - c_2 z_2^2 - c_3 z_3^2 + z_3 z_4 + \delta_n(k_1\dot{z}_1 + k_2\dot{z}_2 + k_3\dot{z}_3 + \dot{z}_4)\\
&= -c_1 z_1^2 - c_2 z_2^2 - c_3 z_3^2 + z_3 z_4 + \delta_n(k_1\dot{z}_1 + k_2\dot{z}_2 + k_3\dot{z}_3 + a_1 x_1 + a_2 x_2 + a_3 x_3\\
&\quad + a_4 x_4 + a_5 u_n + F_1 + c_3\dot{z}_3 + \dot{z}_2 + c_1\ddot{z}_1 - \dddot{x}_d + c_2\ddot{z}_2 + \dddot{z}_1)\end{aligned} \tag{3.9}$$

The backstepping sliding mode control rate of the speed system can be obtained as

$$\begin{aligned}u_n &= \frac{1}{a_5}\Big\{-k_1\dot{z}_1 - k_2\dot{z}_2 - k_3\dot{z}_3 - a_1 x_1 - a_2 x_2 - a_3 x_3 - a_4 x_4 - \overline{F}_1\,\mathrm{sgn}\,(\delta_n)\\
&\quad - c_3\dot{z}_3 - \dot{z}_2 - c_1\ddot{z}_1 + \dddot{x}_d - c_2\ddot{z}_2 - \dddot{z}_1 - h_n[\delta_n + \beta_n\,\mathrm{sgn}\,(\delta_n)]\Big\}\end{aligned} \tag{3.10}$$

where h_n and β_n are positive constants. By introducing equation (3.10) into equation (3.9) we can find

$$\begin{aligned}\dot{v}_4 &= -c_1 z_1^2 - c_2 z_2^2 - c_3 z_3^2 + z_3 z_4 - h_n\delta_n^2 - h_n\beta_n|\delta_n| + F_1\delta_n - \overline{F}_1|\delta_n|\\
&\leqslant -c_1 z_1^2 - c_2 z_2^2 - c_3 z_3^2 + z_3 z_4 - h_n\delta_n^2 - h_n\beta_n|\delta_n| + |\delta_n|(|F_1| - \overline{F}_1)\\
&\leqslant -c_1 z_1^2 - c_2 z_2^2 - c_3 z_3^2 + z_3 z_4 - h_n\delta_n^2 - h_n\beta_n|\delta_n|\end{aligned} \tag{3.11}$$

Define a positive definite matrix $\mathbf{Q}_n$ as follows

$$\mathbf{Q}_n = \begin{bmatrix} c_1 + h_n k_1^2 & h_n k_1 k_2 & h_n k_1 k_3 & h_n k_1 \\ h_n k_1 k_2 & c_2 + h_n k_2^2 & h_n k_2 k_3 & h_n k_2 \\ h_n k_1 k_3 & h_n k_2 k_3 & c_3 + h_n k_3^2 & h_n k_3 - \frac{1}{2} \\ h_n k_1 & h_n k_2 & h_n k_3 - \frac{1}{2} & h_n \end{bmatrix} \tag{3.12}$$

Because

$$\mathbf{Z}^{\mathrm{T}}\mathbf{Q}_n\mathbf{Z} = c_1 z_1^2 + c_2 z_2^2 + c_3 z_3^2 - z_3 z_4 + h_n\delta_n^2 \tag{3.13}$$

and

$$\dot{v}_4 \leqslant -\mathbf{Z}^{\mathrm{T}}\mathbf{Q}_n\mathbf{Z} - h_n\beta_n|\delta_n| \tag{3.14}$$

where

$$|\mathbf{Q}_n| = h_n c_1 c_2(c_3 + k_3) - \frac{c_1 c_2 + h_n(c_2 k_1^2 + c_1 k_2^2)}{4} \tag{3.15}$$

By taking appropriate values of h_n, c_1, c_2, c_3, k_1, k_2, k_3, one can make $|\mathbf{Q}_n| > 0$.
Define an equation

$$w(t) = \mathbf{Z}^{\mathrm{T}}\mathbf{Q}_n\mathbf{Z} + h_n\beta_n|\delta_n| \leqslant -\dot{v}_4(z_1(t)z_2(t)z_3(t)z_4(t)) \tag{3.16}$$

Integrate both sides of equation (3.16) at the same time

$$\begin{aligned}\int_0^t w(\tau)\,d\tau &\leqslant -\int_0^t \dot{v}_4(z_1(\tau)z_2(\tau)z_3(\tau)z_4(\tau))\,d\tau\\
&= v_4(z_1(0)z_2(0)z_3(0)z_4(0)) - v_4(z_1(t)z_2(t)z_3(t)z_4(t))\end{aligned} \tag{3.17}$$

$\lim_{t\to\infty}\int_0^t w(\tau)\,d\tau$ exists and is limited. According to the Barbarat lemma $\lim_{t\to\infty} w(t) = 0$.

So $t \to \infty$, $z \to 0$, $\delta_n \to 0$ and $Y \to x_d$. That is, the system still tends to be stable in the presence of the disturbance.

Because the upper bound of F_1 is uncertain, adaptive control can be used to estimate F_1 (Esmaeili *et al.*, 2019). Let the estimated error be $\widetilde{F}_1$, the estimate $\widehat{F}_1$, then we can obtain

$$\widetilde{F}_1 = F_1 - \widehat{F}_1 \tag{3.18}$$

Define a Lyapunov function

$$v_5 = v_4 + \frac{1}{2\gamma_n}\widetilde{F}_1^2 \tag{3.19}$$

where γ_n is a positive constant

$$\dot{v}_5 = \dot{v}_4 - \frac{1}{\gamma_n}\widetilde{F}_1\dot{\widehat{F}}_1 = \dot{v}_4 - \frac{1}{\gamma_n}\widetilde{F}_1(\dot{\widehat{F}}_1 - \gamma_n\delta_n) \tag{3.20}$$

The ABSMC controller of the speed system can be obtained

$$\begin{aligned} u_n = \frac{1}{a_5}\Big\{ &-k_1\dot{z}_1 - k_2\dot{z}_2 - k_3\dot{z}_3 - a_1x_1 - a_2x_2 - a_3x_3 - a_4x_4 - \widehat{F}_1 - c_3\dot{z}_3 - \dot{z}_2 \\ &- c_1\ddot{z}_1 + \dddot{x}_d - c_2\ddot{z}_2 - \ddot{z}_1 - h_n[\delta_n + \beta_n\,\mathrm{sgn}\,(\delta_n)]\Big\} \end{aligned} \tag{3.21}$$

where

$$\dot{\widehat{F}}_1 = \gamma_n\delta_n \tag{3.22}$$

Bring equations (3.21) and (3.22) into equation (3.20)

$$\dot{v}_5 = -c_1z_1^2 - c_2z_2^2 - c_3z_3^2 + z_3z_4 - h_n\delta_n^2 - h_n\beta_n|\delta_n| = -\mathbf{Z}^{\mathrm{T}}\mathbf{Q}_n\mathbf{Z} - h_n\beta_n|\delta_n| = -w(t) \leqslant 0 \tag{3.23}$$

where $|\mathbf{Q}_n| > 0$. According to the Barbarat lemma $\lim_{t\to\infty} w(t) = 0$. $t \to \infty$, $z \to 0$ so as to ensure the stability of the speed system.

From equation (2.2), it can be obtained that the adaptive backstepping sliding mode controller of the torque system is

$$u_m = \frac{1}{b_4}\Big\{ -l_1\dot{\varepsilon}_1 - l_2\dot{\varepsilon}_2 - b_1x_1 - b_2x_2 - b_3x_3 - \widehat{F}_2 - r_2\dot{\varepsilon}_2 - r_1\ddot{\varepsilon}_1 - \dot{\varepsilon}_1 + \dddot{x}_d - h_m[\delta_m + \beta_m\,\mathrm{sgn}\,(\delta_m)]\Big\} \tag{3.24}$$

where l_1, l_2, r_1, r_2, h_m, β_m are positive constants.

4. Simulation research

The simulation model of the system is established by Matlab Simulink, and the effectiveness of the ABSMC control strategy is verified by comparing the adaptive control strategy. System parameters are shown in Table 1.

After repeated debugging and ensuring that the $\mathbf{Q}_n$ and $\mathbf{Q}_m$ matrices are positive definite, the controller parameters of the speed system are obtained as follows $c_1 = 100$, $c_2 = 50$, $c_3 = 20$, $k_1 = 100$, $k_2 = 50$, $k_3 = 20$, $h_n = 30$, $\beta_n = 10$, $\gamma_n = 600$. The controller parameters of the torque system are $l_1 = 300$, $l_2 = 40$, $r_1 = 300$, $r_2 = 40$, $h_m = 200$, $\beta_m = 20$, $\gamma_m = 2000$.

First, verify the performance of the two systems when the internal parameters of the system change. According to the expression of the speed system, the equivalent moment of inertia mainly
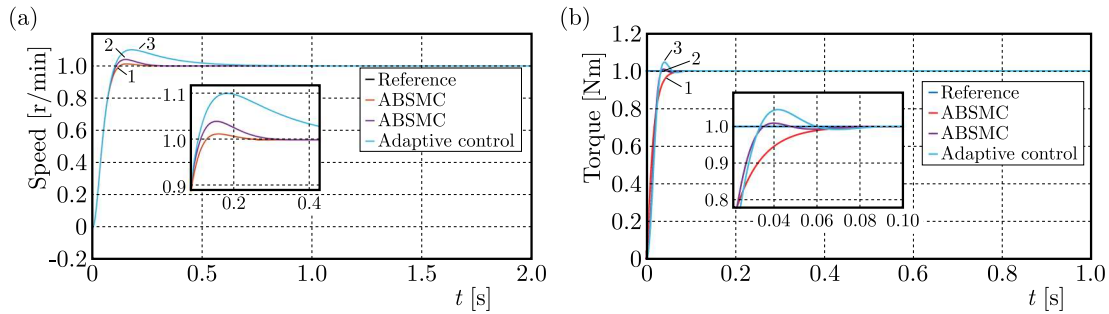
Fig. 2. Step response of: (a) speed system, (b) torque system

affects the speed system. When J_q increases by 5 times, verify the step response of the speed system controlled by ABSMC, as shown in Fig. 2a. Since the torque system is greatly affected by the natural frequency of the electro-hydraulic servo valve, when it is reduced by 50%, verify the step response of the torque system controlled by ABSMC, as shown in Fig. 2b.

It can be seen in Fig. 2a, curve 1 shows a step response of the speed system when $J_q = 1.13\,\text{kg}\,\text{m}^2$, and the overshoot is 1.8%. Curves 2 and 3 show the step response when the system parameters change $J_q = 5.65\,\text{kg}\,\text{m}^2$. When the moment of inertia increases by 5 times, the step response of the speed system is overshoot. Under the adaptive strategy, the system overshoot is 10% and the adajustment time is 0.7 s. Under the control of ABSMC strategy, the system overshoot is 4.1%, the adjustment time is 0.3 s, the speed system overshoot increases slightly, and a change in the steady-state error is small. As shown in Fig. 2b, curve 1 shows the step response of the torque system when $\omega_v = 560\,\text{rad/s}$, and curves 2 and 3 show the step response when $\omega_v = 280\,\text{rad/s}$. The natural frequency of the electro-hydraulic servo valve decreases by 50%, the response of the system becomes faster and the stability becomes worse. In adaptive strategy control, the overshoot of the step response is 5%, the adjustment time is 0.15 s, and there is chattering in the convergence process. For the system controlled by ABSMC, the overshoot of the step response is only 1%, the adjustment time is 0.08 s, and the chattering in the convergence process is small.

Secondly, the performance of the two systems is verified when there is an external coupling interference. The sinusoidal signal with an amplitude of 1 is taken as the reference signal, and the random signal is taken as the external coupling interference of the system. Verify the estimation of random interference by ABSMC strategy, sinusoidal tracking response and tracking error of the two systems. As can be seen in Fig. 3, it shows the response of the speed system.

As shown in Fig. 3a, the random disturbance suddenly changes at 4 s and 8 s. There are errors in the disturbance estimation of adaptive control. The estimation of random disturbance by ABSMC control is fast and accurate. As shown in Fig. 3b and 3c, in adaptive control, the maximum tracking errors are 0.09 r/min and 0.05 r/min, respectively, and the convergence time is 0.4 s. The tracking errors of the system controlled by ABSMC are 0.05 r/min and 0.025 r/min, respectively, the convergence time is only 0.1 s, and the convergence is stable.

As shown in Fig. 4, it is the sinusoidal response of the torque system, and the random disturbance amplitude is greater than that of the speed system.

In the loading experiment, the external force interference of the torque system is greater than that of the speed system. Therefore, the disturbance amplitude of the torque system is greater than that of the speed system. As can be seen in Fig. 4a, the estimation of disturbance by ABSMC control is still accurate. At 4s and 8s, the maximum tracking error of the system controlled by ABSMC is 0.09 Nm and 0.04 Nm, respectively, and the convergence time is only 0.1 s. The ABSMC controller shows good robustness. For small disturbances, the ABSMC controller controls fully and the system runs smoothly, so this paper will not repeat it.
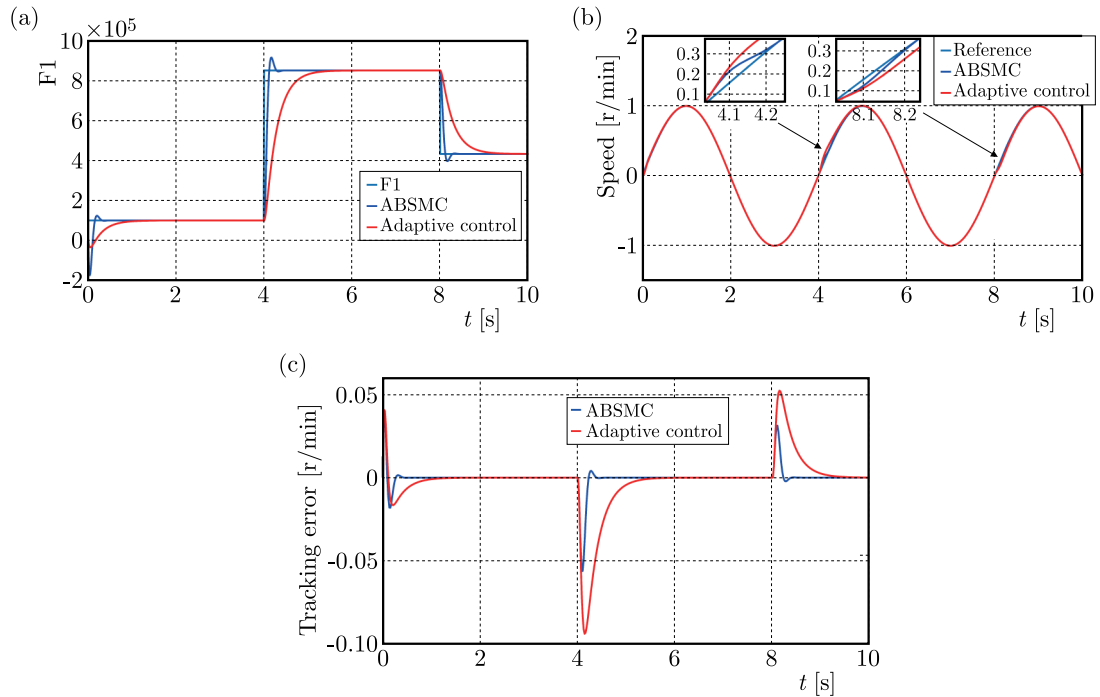
Fig. 3. Speed system simulation curve: (a) disturbance estimation, (b) sinusoidal tracking, (c) tracking error
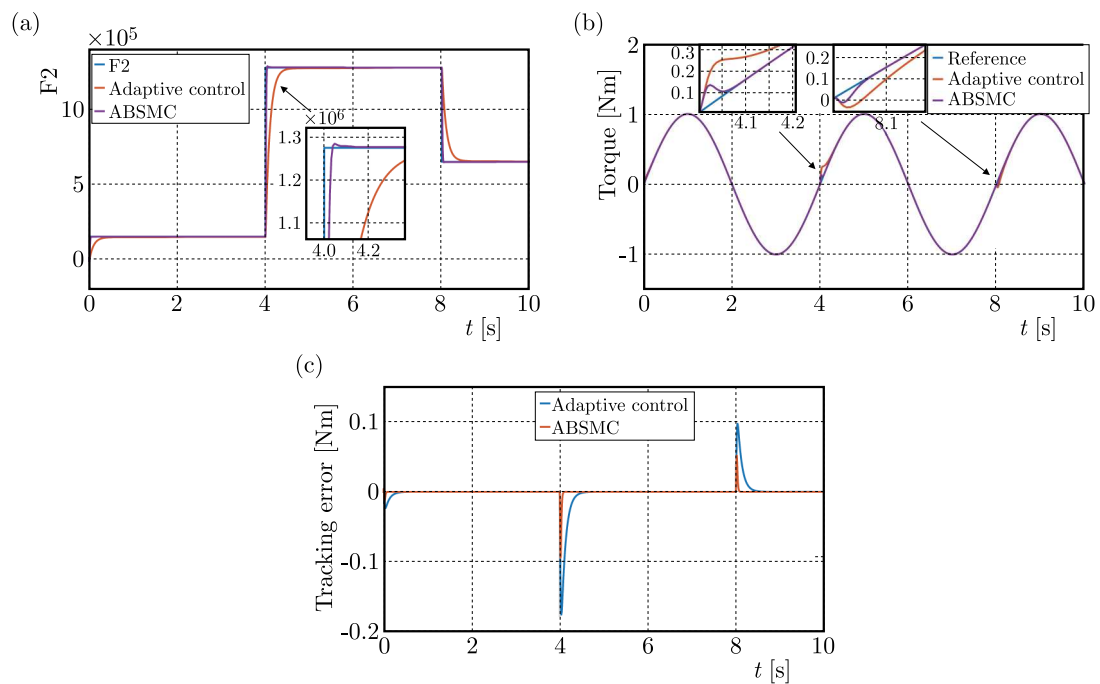

Fig. 4. Torque system simulation curve: (a) disturbance estimation, (b) sinusoidal tracking, (c) tracking error

5.   Experimental research

The vehicle drive axle loading test-bed is composed of a drive speed control system, secondary output loading torque control system and left and right wheel side loading torque control systems. As shown in Fig. 5, the four systems can be adjusted by a controller, respectively.

The computer control system is shown in Fig. 6. The function of the upper computer is to set the test parameters and store the data. The lower computer is composed of an industrial control
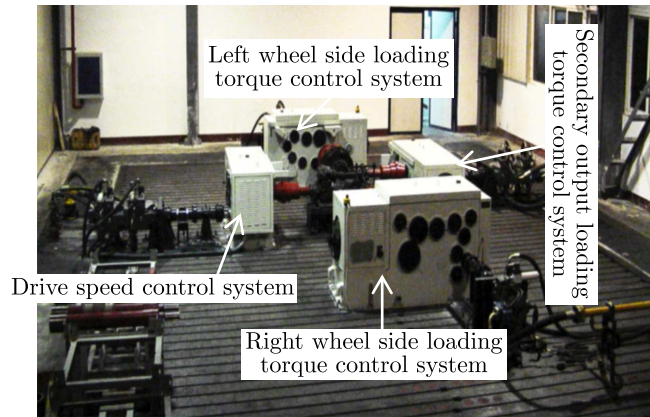
Fig. 5. Photo of the vehicle drive axle loading test bench

computer, data I/O interface board and an AD/DA data acquisition board, which is responsible for measurement of the test parameters and logic control of the test bench. Four HNC-100 controllers are used to realize the internal and external loop control of the four systems. NI-PXI unit is responsible for collecting the parameters of each secondary element and sending them to the lower computer. PLC mainly completes the gear switching of each transmission. The upper computer communicates with the lower computer through Ethernet. The upper computer communicates with PLC through PCI-1602E RS422/RS485 communication card.
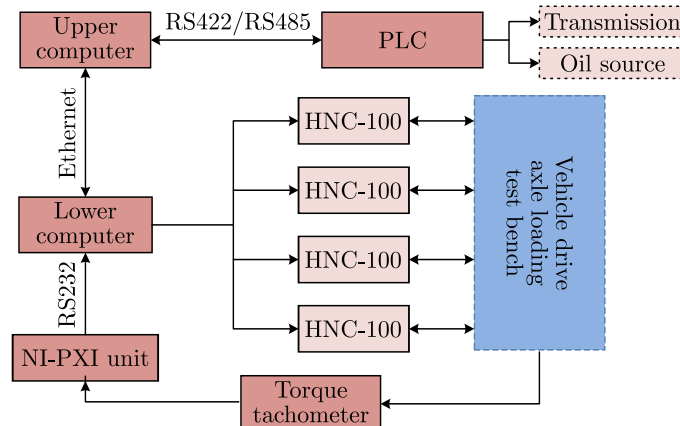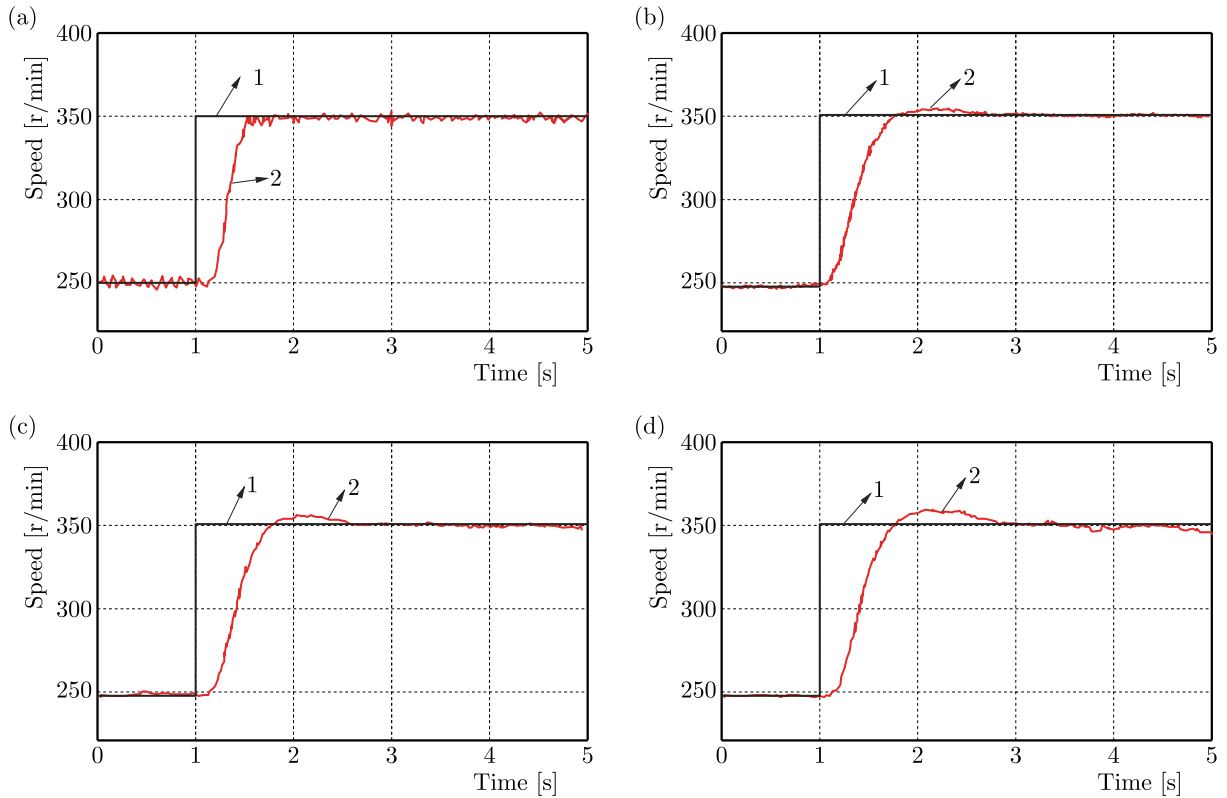

Fig. 6. Computer control system

Because the secondary output loading torque control system has the same performance as the left and right wheel side loading torque control systems, this experiment only studies the drive speed and secondary output loading torque control system. The purpose of the test is to test the anti-interference ability of the drive speed and secondary output loading torque control system by using the designed ABSMC controller.

The wheel axle simulation loading system adjusts the load of the loading object (wheel axle) by driving the transmission (four gears), secondary output transmission (three gears) and the left and right wheel side transmission (three gears). In order to analyze the influence of the equivalent moment of inertia on the performance of the speed system, four different gear combinations are taken for the test, as shown in Table 2.

Figures 7a, 7b, 7c and 7d correspond to working conditions I, II, III and IV, respectively, and the equivalent moment of inertia from small to large is 0.99, 1.13, 1.95 and 5.65 kgm^2, respectively.

Table 2. Influence of rotational inertia on system performance

Working condi- tion	Drive transmis- sion gear	Secondary transmis- sion gear	Left wheel transmis- sion gear	Right wheel transmis- sion gear	J_q [kg m²]	Speed overshoot amount [%]	Speed steady state error [%]
I	1	1	2	2	0.99	1.1	0.9
II	1	1	1	1	1.13	1.8	0.6
III	2	2	1	1	1.95	2.7	0.8
IV	3	2	2	2	5.65	4.1	1.1

Fig. 7. Step response test curve of the speed system

Curves 1 and 2 in the figure are the step input and test output, respectively. It can be seen in Fig. 7 and Table 2 that when $J_q = 1.13\,\text{kg m}^2$, the overshoot is 1.8% and the steady-state error is 0.6%; when $J_q = 5.66\,\text{kg m}^2$, the overshoot is 4.1% and the steady-state error is 1.1%. The overshoot and steady-state error of the speed system increase slightly, which is basically consistent with the simulation results obtained in Fig. 2.

In the computer control system, a random disturbance is input to the speed and torque system, and a sudden change occurs at 10 s to verify the sinusoidal response of the speed and torque systems, as shown in Figs. 8a and 8b. Curves 1 and 2 in the figure are the sinusoidal input and test output, respectively. The amplitude of the sinusoidal signal of input speed and torque systems is 55 r/min and 50 Nm, respectively, and the frequency is 0.1. The random disturbance suddenly changes at 10 s, the maximum tracking error of the speed control system is 0.05 r/min, and the convergence time is 0.1 s.The maximum tracking error of the torque control system is 0.09 Nm, and the convergence time is 0.15 s. This is basically consistent with the conclusion of simulation analysis in Figs. 3 and 4. The ABSMC controller shows good robustness.
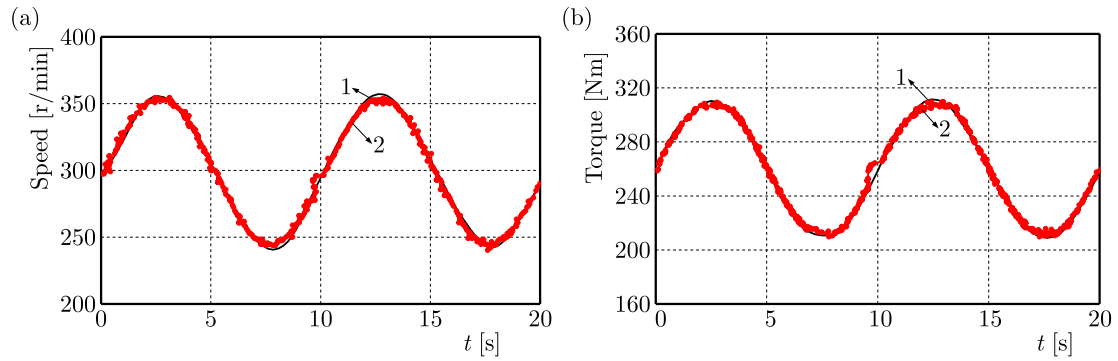
(a)

(b)

Fig. 8. Experimental curve of: (a) speed system, (b) torque system

6. Conclusions

There are parameter disturbances and coupling disturbances in the vehicle drive axle loading test-bed, which have a great impact on the control performance of the system. In this paper, the controller of the test-bed is designed by using the adaptive backstepping sliding mode control strategy, and the performance of the controller is verified by simulation and an experiment. The results show that under the condition of a large parameter disturbance and a random disturbance, the ABSMC controller shows good control performance, and the loading test-bed can still run smoothly. Therefore, the controller designed in this paper provides a good solution for the accuracy control of the vehicle drive axle loading test-bed.

References

1. DING Q., PENG S., QIU L.H., WANG Z.L., TANG Z.Y., 2006, Study on predictive control of secondary regulation loading system (in Chinese), *China Mechanical Engineering*, **17**, 10, 1022-1025

2. ESMAEILI N., KAZEMI R., OREH S., 2019, An adaptive sliding mode controller for the lateral control of articulated long vehicles, *Proceedings of the Institution of Mechanical Engineers*, **233**, 3, 487-515

3. FAJRI P., LEE S., PRABHALA V., FERDOWSI M., 2016, Modeling and integration of electric vehicle regenerative and friction braking for motor/dynamometer test bench emulation, *IEEE Transactions on Vehicular Technology*, **65**, 6, 4264-4273

4. HAN S.B., CHANG Y.H., CHUNG Y.J., LEE E.Y., SUH B., FRAMK A., 2009, Fuel economy comparison of conventional drive trains series and parallel hybrid electric step vans, *International Journal of Automotive Technology*, **10**, 2, 235-240

5. HU J.B., GUO X.L., YUAN S.H., PENG Z.X., 2008, Dynamic characteristics of hydrostatic secondary control load simulation system and the approach to resist load disturbance (in Chinese), *Journal of Agricultural Machinery*, **39**, 6, 150-153

6. HUANG S.J., YANG C.S., 2015, Adaptive functional approximation strategy for a four-wheel drive electrical vehicle driving speed control, *Proceedings of the Institution of Mechanical Engineers, Part I: Journal of Systems and Control Engineering*, **229**, 4, 319-333

7. LAUWERYS C., SWEVERS J., SAS P., 2005, Robust linear control of an active suspension on a quarter car test-rig, *Control Engineering Practice*, **13**, 5, 577-586

8. LI M.X., JIA Y.M., 2017, Decoupling and robust control of velocity-varying four-wheel steering vehicles with uncertainties via solving attenuating diagonal decoupling problem, *Journal of the Franklin Institute*, **354**, 1, 105-122

9. Li M.X., Jia Y.M., Du J.P., 2014, LPV control with decoupling performance of 4WS vehicles under velocity-varying motion, *IEEE Transactions on Control Systems Technology*, **22**, 5, 1708-1724

10. Pang H., Yao R., Wang P., Xu Z., 2021, Adaptive backstepping robust tracking control for stabilizing lateral dynamics of electric vehicles with uncertain parameters and external disturbances, *Control Engineering Practice*, **110**, 4, 104-116

11. Peng J., He H., Feng N., 2013, Simulation research on an electric vehicle chassis system based on a collaborative control system, *Energies*, **6**, 1, 312-328

12. Shen W., Huang H., Pang Y., Su X., 2017, Review of the energy saving hydraulic system based on common pressure rail, *IEEE Access*, **5**, 655-669

13. Song J.C., Ju Y.F., 2020, Distributed adaptive sliding mode control for vehicle platoon with uncertain driving resistance and actuator saturation, *Complexity*, **20**, 1-12

14. Su D.H., Wang M.X., 2006, Application of modern control theory in secondary speed regulation system (in Chinese), *Machine tool and hydraulic*, **05**, 120-121

15. Wang H., Wang L., Lin Y.H., Yao J.H., 2018, Application of sliding mode control in servo loading systems with secondary regulation (in Chinese), *Control Engineering*, **25**, 11, 1971-1975

16. Zang F.Y., Wang Y., Kong X.Z., 2014, Fuzzy-neural network control on secondary hydraulic transmission system, *Advanced Materials Research*, **945-949**, 1615-1618

17. Zang F.Y., Wang Y., Yang R.M., 2016, Robust control for a class of secondary regulation rotate speed systems via Hamiltonian function method, *Journal of Intelligent and Fuzzy Systems*, **32**, 1, 991-997

18. Zhai L., Sun T., Jie W., 2016, Electronic stability control based on motor driving and braking torque distribution for a four in-wheel motor drive electric vehicle, *IEEE Transactions on Vehicular Technology*, **65**, 6, 4726-4739